metry. The MO results reduce to several approximate descriptions of framework bonding, facilitated in part by the nil interaction (essentially zero overlap population) between Nb atoms, no two of which are closer than 3.39 Å. Basal atoms Nb(2-6) can be viewed as being in square-pyramidal NbS_5 units[53] with a σ-bonding framework consisting of Nb(V) dsp^3 + S^{2-} s/p hybrid orbital interactions. For the apical Nb(1)S_5 portion a fragment analysis was performed. The five μ_3-S atoms can be considered to contribute one sp^3-like orbital each, with the set tranforming as $a_1 + e_1 + e_2$. These mix with metal orbitals of the same symmetry, affording 5 fragment orbitals filled with 10 electrons. The bonding interactions are similar to those in certain boranes and carboranes of fivefold symmetry.[54] Bonding is completed at Nb(1) by σ- and π-bond formation with the atom S_t by use of a_1 and e_1 orbitals, respectively. Similar π bonding occurs at basal Nb atom sites. Overlap populations vary as Nb-S distances. Those involving terminal atoms are consistent with an effective double bond Nb=S, which has been detected in the infrared spectrum.

Other than its framework topology, the most intriguing feature of $[M_6S_{17}]^{4-}$ is the presence of atom S_b within the cage. Designation of this atom as, functionally, μ_6-S on the basis of M-S_b distances is further supported by the overlap populations of 0.23 and 0.11 for the interactions with apical and basal Nb atoms, respectively. To derive a bonding description, a fragment analysis was performed with S_b^{2-} and $[Nb_6S_{16}]^{2-}$, which retains C_{5v} symmetry. In the hypothetical reaction (3) the product is *stabilized*

$$[Nb_6S_{16}]^{2-} + S^{2-} \rightarrow [Nb_6S_{17}]^{4-} \quad (3)$$

by 1.90 eV over the fragments. Further, the LUMO-HOMO separation increases from 1.11 eV in the fragment to 1.60 eV in the product. In both species the HOMO has a_2 symmetry and thus cannot interact with S_b (Table IV). The fragment LUMO is of a_1 symmetry. Its antibonding interaction with the S_b a_1 orbitals drives its energy above that of the e_2 orbital set next to it, which becomes the LUMO of $[Nb_6S_{17}]^{4-}$. This ion has been further fragmented into Nb_6S_b for the purpose of the bonding analysis.

Leading results of the interactions of the orbitals of the six Nb(V) atoms with the orbitals of S_b^{2-} are displayed in Figure 6. Four bonding orbitals are filled, affording the configuration $(1a_1)^2(1e_1)^4(2a_1)^2$. Simplified depictions of these orbitals, showing principal atomic contributions, are provided. The fragment orbitals are mixed with other sulfur orbitals in the complete anion. It is noteworthy that the overlap populations between S_b and the apical and basal Nb atoms, 0.23 and 0.11, respectively, are very close to the values for $[Nb_6S_{17}]^{4-}$ itself. Thus, in spite of its simplicity, the fragment analysis provides a reasonable first approach to a description of the bonding of the S_b atom to the cage framework. The apparent spontaneity of reaction 3 is now interpretable in terms of the formation of four additional filled bonding MO's upon insertion of S_b^{2-} in the precursor cage. The interior of this cage can be conceived of in terms of virtual metal orbitals directed toward its center or along its roof. Hence, the interior is acidic or electron deficient, a condition that is attenuated by the binding of a suitable ligand. This situation is quite prevalent in polyoxometalates,[24] where atoms with high bridging multiplicities enclosed within metal-oxo cages are often encountered. The previously cited ions $[M_6O_{19}]^{2-,8-}$, with μ_6-O atoms in M_6O_{12} cages,[43] are cases in point. With $[M_6S_{17}]^{4-}$ the cage is not closed, and it remains to be seen if an extensive chemistry of open cages with and without interior occupation can be developed. Such chemistry may be expected with complexes of the early transition elements, inasmuch as these metals furnish the required empty and relatively stable d orbitals.

Acknowledgment. This research was supported by NSF Grant CHE 81-06017. X-ray and NMR equipment used in this research were obtained by NSF Grants CHE 80-00670 and CHE 80-08891. We thank Dr. Jay R. Dorfman for useful discussions.

Registry No. $(Et_4N)_4[Nb_6S_{17}]\cdot 3CH_3CN$, 95979-72-9; $(Et_4N)_4[Ta_6S_{17}]\cdot 3CH_3N$, 95979-75-2; $(Me_3Si)_2S$, 3385-94-2.

Supplementary Material Available: Listings of atom coordinates and anisotropic temperature factors for cations and solvate molecules, anisotropic temperature factors for $[M_6S_{17}]^{4-}$, hydrogen atom coordinates and isotropic temperature factors, ranges of atom deviations from and dihedral angles between unweighted least-squares planes of $[M_6S_{17}]^{4-}$, and calculated and observed structure factors for $(Et_4N)_4[M_6S_{17}]\cdot 3MeCN$ (M = Nb, Ta) (80 pages). Ordering information is given on any current masthead page.

(53) For an analysis of C_{4v} ML_5 fragments, cf.: Elian, M.; Hoffmann, R. *Inorg. Chem.* **1975**, *14*, 1058.
(54) Hoffmann, R.; Lipscomb, W. N. *J. Chem. Phys.* **1962**, *36*, 2179.
(55) In this paper the periodic group notation is in accord with recent actions by IUPAC and ACS nomenclature committees. A and B notation is eliminated because of wide confusion. Groups IA and IIA become groups 1 and 2. The d-transition elements comprise groups 3 through 12, and the p-block elements comprise groups 13 through 18. (Note that the former Roman number designation is preserved in the last digit of the new numbering: e.g., III → 3 and 13.)

Notes

Contribution from the Department of Chemistry, University of Leuven, Celestijnenlaan 200F, B-3030 Heverlee, Belgium

Excited-State Spectroscopy of Tetrachloroplatinate(II)

L. Viaene,[1a] A. Ceulemans,*[1b] and L. G. Vanquickenborne[1b]

Received September 12, 1984

In this paper we report the transient absorption spectrum of the tetrachloroplatinate(II) anion in a matrix of ethylene glycol and water at 158 K. The spectrum could be identified as the excited-state absorption (ESA) of $PtCl_4^{2-}$ in its lowest triplet state. This assignment is shown to be consistent with a detailed analysis of the doubly excited ligand field states in a d^8 square-planar complex. The present work follows a methodology that is similar to an earlier treatment, reporting the ESA spectrum of the lowest excited triplet in $Co(CN)_6^{3-}$, and d^6 octahedral complex.[2]

Transient Detection

A 10^{-2} M solution of K_2PtCl_4 in a 2:1 mixture of ethylene glycol and water, containing an excess of KCl, was cooled down to 158 K and excited at 347 nm with a pulsed ruby laser source. The details of the measurement have been described elsewhere.[2] In emission one readily observes a broad-band luminescence peaking at about 12 150 cm^{-1} (see Figure 1). Moreover, a well-structured transient absorption could be monitored from 16 500 to 33 000 cm^{-1}. Traces of transient absorption were also detectable at the low-energy side of the emission peak.

Since the parent compound is not transparent in the region above 17 000 cm^{-1}, the absorption observed immediately after excitation had to be corrected for the transient depletion of the ground state. In Figure 1 this corrected absorbance is plotted against wavenumber. Four main bands at 8400, 18 150, 25 600, and 30 000 cm^{-1} have been labeled from I to IV. Assuming a unit

(1) (a) Laboratory of Inorganic and Analytical Chemistry. (b) Laboratory of Quantum Chemistry.
(2) Viaene, L.; D'Olieslager, J.; Ceulemans, A.; Vanquickenborne, L. G. *J. Am. Chem. Soc.* **1979**, *101*, 1405.

0020-1669/85/1324-1713$01.50/0

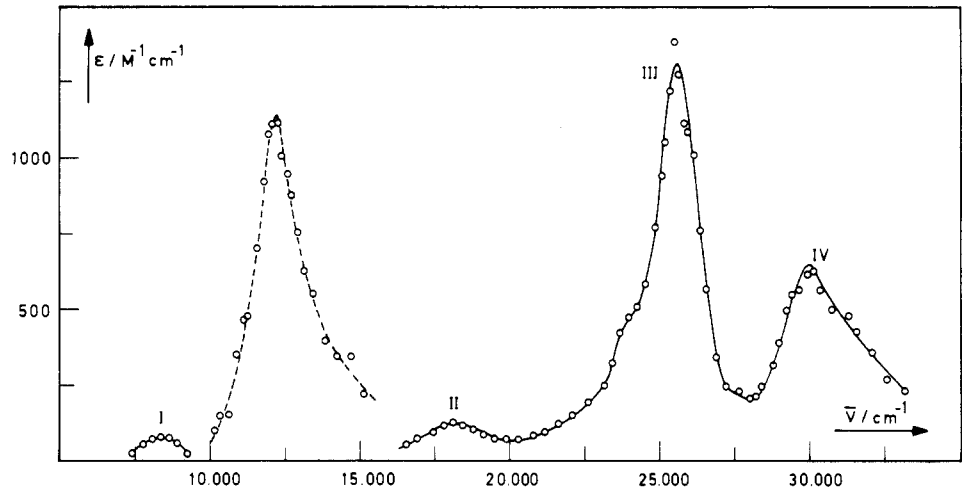

Figure 1. Excited-state absorption spectrum (solid line) of the $PtCl_4^{2-}$ anion in a matrix of ethylene glycol and water at 158 K. The spectrum was corrected for transient depletion of the ground state. No absorption could be recorded between 10 000 and 15 000 cm^{-1} due to a strong emission signal, centered around 12 500 cm^{-1} (dashed line). Extinction coefficient values refer to the ESA spectrum. Emission intensity is in arbitrary units.

efficiency for transient photoproduction, approximate molar extinction coefficients could be calculated. They range from 100 to 1300 M^{-1} cm^{-1}, to be compared with ϵ values of 20–60 M^{-1} cm^{-1} for the ground-state spectrum at 158 K. Both emission and absorption signals proved to obey a strict first-order decay law, characterized by exactly the same rate constant of 2.5 10^5 s^{-1} (τ = 4 μs). Finally, we note that even after prolonged irradiation the original amount of K_2PtCl_4 was restored within the limits of detection.

Nature of the Intermediate

The emission spectrum in frozen solutions closely corresponds to the published emission spectrum of K_2PtCl_4 powder at low temperature, which has been identified as phosphorescence from the lowest triplet excited state of the $PtCl_4^{2-}$ anion to the closed-shell singlet ground state.[3] The measured lifetime of ca. 4 μs is compatible with this assignment.[4] In the absence of any net photochemistry, the fact that the absorption spectrum is characterized by exactly the same lifetime strongly suggests that it originates from the same triplet state. Hence, we assign the spectrum in Figure 1 to the excited-state absorbance of the metastable emitting triplet state of the complex ion. Remark that an entirely analogous proposal for the transient spectrum in $Co(CN)_6^{3-}$ has been based on parallel observations, i.e. absence of photochemistry and identical lifetime for transient emission and absorption.[5]

The detailed nature of the emitting state in $PtCl_4^{2-}$ has extensively been studied by Zink, Gliemann, et al.[6] A Franck–Condon analysis of the single-crystal-polarized luminescence spectra of K_2PtCl_4 and the analogous K_2PtBr_4 lead these authors to the following conclusions: (i) The emitting state is significantly distorted along the totally symmetric stretching coordinate. Pt–Cl bond lengths in the excited state are about 0.1 Å larger than in the ground state. (ii) The corresponding Stokes shift is in the order of 4000 cm^{-1}. (iii) There is no evidence for symmetry-lowering distortions. The excited state is assumed to retain D_{4h} symmetry. (iv) The band polarization is compatible with an emitting state of Γ_1, Γ_3, or Γ_5 symmetry[7] (Bethe notation for spin–orbit components in D_{4h}). A Γ_5 assignment was considered the more probable in view of the measured π/σ polarization ratio.[8]

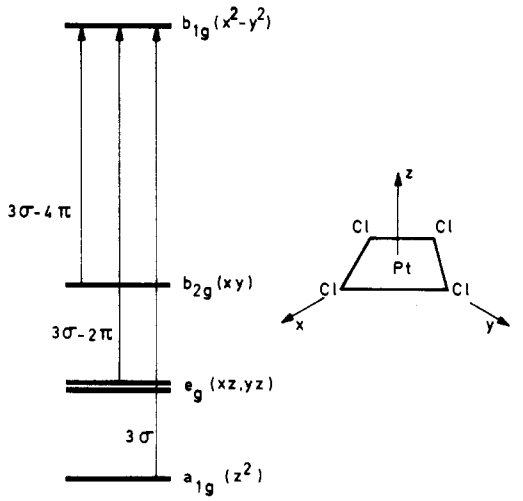

Figure 2. Orbital energy diagram for $PtCl_4^{2-}$. Ligands are on the cartesian x and y axes. Energy expressions for transitions to the b_{1g} orbital were taken from ref 10. These expressions take into account the effect of d–s mixing on the position of the a_{1g} level.

Strictly speaking, these conclusions all refer to the crystalline state. However, because of the pronounced similarity of emission spectra in K_2PtCl_4 powder and in glassy media, it is quite reasonable to expect the same conclusions to hold in frozen solutions as well. In contrast in a Cs_2ZrCl_6 host lattice the $PtCl_4^{2-}$ ion exhibits an entirely different emission spectrum, in all probability due to a different emitting state.[9]

Ligand Field Analysis

The ground-state spectrum of $PtCl_4^{2-}$ shows three types of electronic excitations: ligand field d–d transitions;[10-12] metal-centered d–p transitions; ligand-to-metal charge-transfer (LMCT) bands.[13,14] The spectral characteristics of the ESA do not seem

(3) Webb, D. L.; Rossiello, L. A. *Inorg. Chem.* **1970**, *9*, 2622.
(4) Fleischauer, P. D.; Adamson, A. W.; Sartori, G. *Prog. Inorg. Chem.* **1972**, *2*, 1–56.
(5) The emission lifetime of $Co(CN)_6^{3-}$ in an EPA matrix at 94 K has only recently been shown to be identical with the reported[2] ESA lifetime under the same conditions: Viaene, L., unpublished results.
(6) Yersin, H.; Otto, H. Zink, I. J.; Gliemann, G. *J. Am. Chem. Soc.* **1980**, *102*, 951.
(7) Martin, D. S. *Inorg. Chim. Acta Rev.* **1971**, *5*, 107.
(8) The emission is most intense in π polarization. According to Yersin et al. this is in accordance with a $\Gamma_5 \rightarrow \Gamma_1$ assignment.[6] Note, however, that the $\Gamma_1 \rightarrow \Gamma_5$ (^1E_g) absorption band in the ground-state spectrum is about equally intense in π and σ polarization. See: Moncuit, C. *Theor. Chim. Acta* **1975**, *39*, 255.
(9) Patterson, H. H.; Godfrey, J. J.; Kahn, S. M. *Inorg. Chem.* **1972** *11*, 2872.
(10) Vanquickenborne, L. G.; Ceulemans, A. *Inorg. Chem.* **1981**, *20*, 796.
(11) Martin, D. S.; Tucker M. A.; Kassman, A. J. *Inorg. Chem.* **1965**, *4*, 1682; **1966**, *5*, 1298.
(12) Tuszynski, W. Gliemann, G. *Z. Naturforsch., A: Phys., Phys. Chem., Kosmophys.* **1979**, *34A*, 211.
(13) Isci, H.; Mason, W. R. *Inorg. Chem.* **1984**, *23*, 1565.

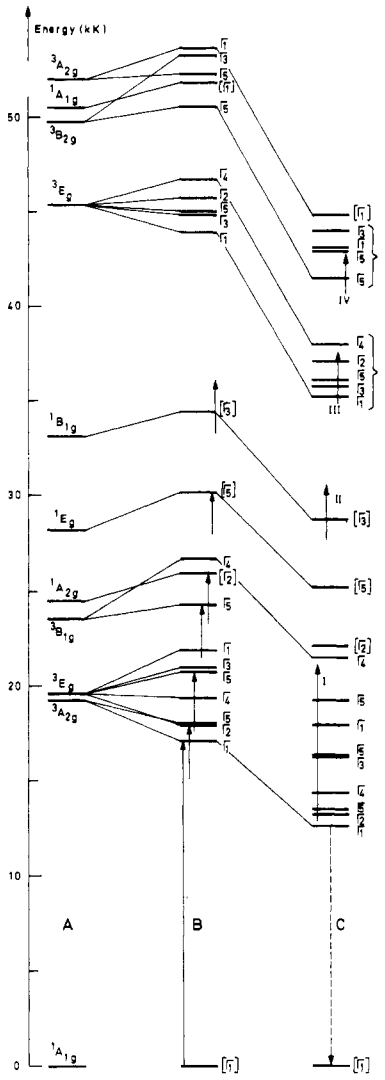

Figure 3. Comparison of calculated and observed d–d transitions in $PtCl_4^{2-}$. (A) Electronic states that result from a ligand field calculation not including spin–orbit coupling. Parameter values: σ = 12 420 cm^{-1}, π = 2800 cm^{-1}, B = 600 cm^{-1}, C = 2400 cm^{-1}. (B) Effect of the spin–orbit coupling taken into account using a ζ parameter of 2700 cm^{-1} (see ref 10). The resulting states are denoted by Bethe labels Γ_1–Γ_5. Labels in square brackets correspond to states of dominant singlet character. The tops of the vertical arrows represent the reported absorption bands for the ground-state spectrum of $PtCl_4^{2-}$. (C) Stokes shift of approximately 4000 cm^{-1} introduced by lowering the values of the σ and π parameters (σ = 10 485 cm^{-1}, π = 2365 cm^{-1}). The lowest excited triplet state is seen to have Γ_1 symmetry. Transient absorption bands originating from this Γ_1 are indicated by vertical arrows numbered from I to IV (cf. Figure 1). The dashed vertical line represents the observed emission band.

to be compatible with either a d–p or a LMCT assignment. Indeed, in the ground-state spectrum these transitions are at least 1 order of magnitude more intense than the ESA bands and have a much larger band width.[13] An assignment of the transient absorption to d–d transitions thus seems to be a more plausible alternative. This proposal will now be examined in the framework of ligand field theory.

A. Ground-State Spectrum. The d-orbital splitting in a square-planar complex[10] is shown in Figure 2. In the ground state of a d^8 complex ion the four low-lying d orbitals are occupied while the σ-antibonding b_{1g} orbital is empty. Singly excited configurations involve all possible one-electron transitions to the b_{1g} orbital. The six corresponding states $^{1,3}B_{1g}$, $^{1,3}E_g$, $^{1,3}A_{2g}$ are shown in the part of the energy diagram in Figure 3A. These levels are further resolved into some 12 spin–orbit components, several of which have unambiguously been assigned through various spectroscopical techniques. A complete spectral fitting thus involves three types of energy parameters: the orbital parameters σ and π, as defined in Figure 2; the interelectronic repulsion parameters B and C; the spin–orbit coupling parameter ζ. Figure 3B resumes the observable transitions as compared to the results of a recent ligand field calculation[10] based on the parameter values σ = 12 420 cm^{-1}, π = 2800 cm^{-1}, B = 600 cm^{-1}, C = 2400 cm^{-1}, and ζ = 2700 cm^{-1}. With this parameter set, highly excited states due to two-electron jumps are predicted in the far-UV region of the spectrum. The states that have been indicated in Figure 3A correspond to the following doubly excited configurations:

$$^3E_g\ (b_{2g} \rightarrow b_{1g};\ e_g \rightarrow b_{1g})$$

$$^3B_{2g}\ (b_{2g} \rightarrow b_{1g};\ a_{1g} \rightarrow b_{1g})$$

$$^3A_{2g}\ (e_g \rightarrow b_{1g};\ e_g \rightarrow b_{1g})$$

$$^1A_{1g}\ (b_{2g} \rightarrow b_{1g};\ b_{2g} \rightarrow b_{1g}) \qquad (1)$$

None of these states are actually observable in the ground-state spectrum, because of the occurrence in the same energy region of far more intense dipole-allowed LMCT and d–p transitions.

B. Excited-State Spectrum. A ligand field analysis of the excited-state spectrum clearly will require a modified parameter set to cope with the increase of the equilibrium distance in the metastable absorbing state. A quantitative estimate of the effect of distortional relaxation can be obtained from the Stokes shift.[2] Presumably, the atomic parameters B, C, and ζ will be rather insensitive to small changes of M–L distance, so that nearly the complete Stokes shift should be due to a decrease of the ligand field parameters σ and π. In the case of $PtCl_4^{2-}$ the orbital energy gap between the ground state and the lowest excited configuration $b_{2g} \rightarrow b_{1g}$ (see Figure 2) precisely corresponds to the spectrochemical strength parameter $10Dq = 3\sigma - 4\pi$. A Stokes shift of roughly 4000 cm^{-1} therefore should imply an equal loss of field strength upon elongation of the Pt–Cl bond. Reducing $10Dq$ from 26 060 cm^{-1} in the ground state to 22 000 cm^{-1} in the metastable excited state, while leaving the σ:π ratios unaltered, then yields the orbital parameters σ = 10 485 cm^{-1}, π = 2365 cm^{-1}. Figure 3C represents the results of an energy calculation, based on these new σ and π values, whereas the B, C, and ζ parameters were left unchanged.

The lowest excited state of the distorted configuration appears to be a totally symmetric Γ_1 state of mixed ^3E_g and $^3A_{2g}$ parentage in a 2:1 ratio. As compared to the ground-state spectrum (Figure 3B) this state is Stokes shifted over about 4500 cm^{-1}. The Γ_1 symmetry is compatible with the polarization measurements of Yersin et al. although these authors advocated a Γ_5 symmetry assignment.[6,8] $\Gamma_1 \rightarrow \Gamma_1$ emission is allowed in π polarization via vibronic coupling to an a_{2u} vibrational mode and in σ polarization via coupling to e_u modes.[7]

In Figure 3C the four experimental ESA bands, numbered I through IV (Figure 1), have been represented by vertical arrows, based on the lowest triplet Γ_1 as the metastable absorbing state. This diagram suggests a straightforward correspondence between the two most prominent ESA bands, III and IV, and two spin-allowed triplet–triplet transitions to spin–orbit components of respectively ^3E_g and $^3A_{2g}$, $^3B_{2g}$ character. Compared with Figure 3B these highly excited levels appear to be lowered in energy to a considerable extent, which explains the spectral separation of LMCT and doubly excited d–d states in the ESA spectrum.

The weak ESA signal at 18 150 cm^{-1} (band II) coincides with the spin-forbidden triplet–singlet $\Gamma_1 \rightarrow [\Gamma_3]$ transition. Finally, the lowest ESA band at 8400 cm^{-1} (band I) probably can be identified as a $\Gamma_1 \rightarrow \Gamma_4$ transition. We note that the intensity of this band is comparable to the intensity of the spin-allowed d–d transitions in the ground-state spectrum.[15]

(14) Kozelka, J.; Ludwig, W. *Helv. Chim. Acta* **1983**, *66*, 902.

(15) Another weak absorption of $\Gamma_1 \rightarrow [\Gamma_5]$ nature is predicted at 12 500 cm^{-1}. This spectral region could not be investigated since it overlaps with the emission signal.

Obviously, the other ESA bands are considerably more intense. Similar intensity discrepances between excited-state and ground-state spectra have been noted[2] in the case of $Co(CN)_6^{3-}$. Probably in the ESA spectrum the vibronic mechanism of d-d intensity is more effective due to the vicinity of strongly allowed LMCT or d-p bands.

In conclusion, a ligand field analysis seems to confirm kinetic evidence for the ESA nature of the reported transient spectrum. Reasonable estimates of the prominent ESA peaks could be obtained by taking the Stokes shift as a measure for the decrease in ligand field strength upon relaxation to the metastable state.

Acknowledgment. A.C. is indebted to the National Fonds voor Wetenschappelijk Onderzoek for a research associate grant.

Registry No. $PtCl_4^{2-}$, 13965-91-8.

Contribution from the Department of Chemistry, University of Georgia, Athens, Georgia 30602

Chemical Applications of Topology and Group Theory. 18. Polyhedral Isomerizations of Seven-Coordinate Complexes[1]

R. B. King

Received July 30, 1984

A topic of considerable interest to inorganic chemists is the stereochemical nonrigidity in ML_n coordination complexes (M = central atom, generally a metal; L = ligands surrounding M). Several theoretical approaches have been used to study such stereochemical nonrigidity. Thus, selected types of possible isomerizations of ML_n polyhedra [$n = 4$,[2] 5,[3] 6,[4] and 8[5]] have been represented topologically[2,6] as graphs in which the vertices represent different polyhedral isomers and the edges represent possible one-step isomerizations. Selected individual polyhedral isomerizations have been described in terms of processes originally called diamond-square-diamond (dsd) processes[7] but can be more systematically called 4-pyramidal processes.[8] A recent paper of this series[8] used Gale transformations[9] to find all possible nonplanar isomerization processes for polyhedra having five and six vertices. By this approach all degenerate nonplanar isomerizations of five-vertex polyhedra were shown to be formulated as sequences of Berry pseudorotation processes, the prototypical dsd or 4-pyramidal process. Furthermore, study of the Gale transformations reveals that degenerate nonplanar isomerizations of the seven combinatorially distinct six-vertex polyhedra can be expressed in terms of six distinct types of 4-pyramidal processes and the two prototypical 5-pyramidal processes.

The success of the Gale transformation approach for the study of polyhedral isomerizations lies in the ability of Gale transformations to reduce the dimensionality of the problem. Thus, the Gale transform of a (three-dimensional) polyhedron having v vertices can be imbedded into $(v-4)$-dimensional space.[8] The Gale transform of a tetrahedron is thus a single point, the Gale transform of a five-vertex polyhedron (trigonal bipyramid or square pyramid) consists of points on a line, and the Gale transform of any of the seven six-vertex polyhedra consists of points in a plane. This dimensionality reduction is the key to the value of Gale transforms in the study of isomerizations of polyhedra with "few" vertices[9] (i.e., ≤ 6 vertices).

Polyhedra having more than six vertices are also of interest to inorganic chemists. However, Gale transformations offer no advantage for the study of the isomerizations of such polyhedra since they no longer provide dimensionality reduction (i.e., for $v > 6$, $v-4 \geq 3$). However, the experience provided by the Gale transformation study of five- and six-vertex polyhedra[8] coupled with the still manageable number of combinatorially distinct seven-vertex polyhedra, namely 34,[10] allows an exhaustive study of isomerizations of seven-vertex polyhedra. This paper summarizes the results of such a study. Polyhedra having seven vertices are of interest in representing the coordination polyhedra of the large variety of known ML_7 complexes.[11]

Background

A polyhedral isomerization step may be defined[6] as a deformation of a specific polyhedron P_1 to the point that the vertices define a new polyhedron P_2. Of particular interest in the context of this work are sequences of two polyhedral isomerization steps $P_1 \rightarrow P_2 \rightarrow P_3$ with the following properties: (a) P_3 has the same number of edges as P_1. (b) P_2 has one less edge than P_1 (or P_3). Such a polyhedral isomerization can be considered to result from removal of one edge from P_1 to give P_2 followed by adding the edge back to P_2 in a different way to give P_3. Note that by definition all polyhedra involved in a sequence of isomerization steps must have the same number of vertices. If P_1 and P_3 are combinatorially equivalent, the polyhedral isomerization $P_1 \rightarrow P_2 \rightarrow P_3$ is called a *degenerate* polyhedral isomerization.

Let us now consider the effects of edge removal from P_1 on the face structure of the resulting polyhedron P_2. Removal of a single edge will convert two faces into a single larger face, which can be called the *pivot* face. If the pivot face has n edges, then the process $P_1 \rightarrow P_2 \rightarrow P_3$ defined as above will be an n-pyramidal process. Note that, for rearrangements of polyhedra having v vertices, the admissible values for n are $4 \leq n \leq v$. A v-pyramidal polyhedral isomerization of a v-vertex system is a *planar* polyhedral isomerization since the intermediate "polyhedron" P_2 is actually a planar polygon with v vertices.

These concepts may be illustrated more concretely. A 4-pyramidal process involves removal and subsequent addition of an edge in the following way so that P_1 and P_3 have the same number of edges:

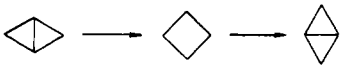

(1)

This, of course, is the familiar dsd process.[7,12] A 5-pyramidal process merges adjacent triangle and quadrilateral faces into a pentagonal face in the intermediate polyhedron P_2 as follows:

(2)

An example of this type of process is described in the Gale diagram paper.[8] The 4-pyramidal and 5-pyramidal processes (1) and (2) can be combined to give the following process:

(3)

In this process (eq 3), *two* edges are removed from P_1 to give P_2 and those two edges are added back to P_2 in a different way to

(1) Part 17. King, R. B. *Theor. Chim. Acta*, in press.
(2) Muetterties, E. L. *J. Am. Chem. Soc.* **1969**, *91*, 1636.
(3) Brocas, J. *Top. Curr. Chem.* **1972**, *32*, 43.
(4) Muetterties, E. L. *J. Am. Chem. Soc.* **1968**, *90*, 5097.
(5) King, R. B. *Theor. Chim. Acta* **1981**, *59*, 25.
(6) Klemperer, W. G. *J. Am. Chem. Soc.* **1972**, *94*, 6940.
(7) Lipscomb, W. N. *Science (Washington, D.C.)* **1966**, *No. 153*, 373.
(8) King, R. B. *Theor. Chim. Acta* **1984**, *64*, 439.
(9) Grünbaum, B. "Convex Polytopes"; Interscience: New York, 1967.
(10) Federico, P. J. *Geometriae Dedicata* **1975**, *3*, 469.
(11) Kepert, D. L. *Prog. Inorg. Chem.* **1979**, *25*, 42.
(12) King, R. B. *Inorg. Chim. Acta* **1981**, *49*, 237.

0020-1669/85/1324-1716$01.50/0